Article:

Song, X., Han, D., Shi, L. orcid.org/0000-0002-1200-8160 et al. (2 more authors) (2025) Energy efficiency maximization for a relay assisted parasitic symbiotic radio network. IET Communications, 19 (1). e70058. ISSN 1751-8628

https://doi.org/10.1049/cmu2.70058

IET Communications

ORIGINAL RESEARCH OPEN ACCESS

Energy Efficiency Maximization for a Relay Assisted Parasitic Symbiotic Radio Network

Xi Song[1] | Dongsheng Han[1] | Liqin Shi[2] | Yinghui Ye[2] | Xiaoli Chu[3]

[1]School of Electrical and Electronic Engineering, North China Electric Power University, Baoding, China | [2]Shaanxi Key Laboratory of Information Communication Network and Security, Xi'an University of Posts and Telecommunications, Chang'an West Street, Xi'an, China | [3]Department of Electronic and Electrical Engineering, The University Of Sheffield, Sheffield, UK

Correspondence: Liqin Shi (liqinshi@hotmail.com)

Received: 19 July 2024 | **Revised:** 1 April 2025 | **Accepted:** 5 June 2025

Funding: This research is supported by the National Natural Science Foundation of China (62301421).

ABSTRACT

Relay-assisted symbiotic radio (SR) has been recently proposed to overcome the blocking of the direct link from the primary transmitter (PT) or backscatter node (BN) to the destination node (DN). However, the energy efficiency (EE), which is an important performance metric for SR networks, has been largely ignored in existing studies of the relay-assisted SR. To fill the gap, this work maximizes the EE of a relay-assisted parasitic SR network, which comprises a PT, a BN, a relay node (RN), and a DN. More specifically, we formulate a mixed-integer programming optimization problem that maximizes the system EE by jointly optimizing the transmit power of the PT, the power reflection coefficient of the BN, the transmit power and the power allocation ratio at the RN as well as the successive interference cancellation (SIC) decoding order at the DN. We decompose the formulated non-convex problem into two subproblems corresponding to the two different SIC decoding orders, respectively. For each subproblem, we convert its objective function from a fractional form into a subtractive form by using a Dinkelbach-based method, and then utilize the block coordinate descent (BCD) method to further decouple it into two subsubproblems that are proved to be convex. Based on the obtained solutions, we devise an iterative algorithm to solve each subproblem by solving its two subsubproblems alternately. The optimal solution to the subproblem with a higher system EE returns a near-optimal solution to the original problem. Simulation results demonstrate the rapid convergence of the proposed algorithms and validate the significant advantages of our proposed algorithms over the baseline schemes.

1 | Introduction

With the ongoing advancement of Internet of Things (IoT) technology, there emerges the prospect of a broader and more extensive wireless connectivity among massive devices [1, 2]. This engenders two key challenges for IoT development, that is, the limited spectrum resources and the constrained battery capacity of IoT nodes [3]. To address these two challenges, ambient backscatter communication (AmBC) has been considered as a promising solution [4, 5]. Specifically, in AmBC, the IoT device (also namely backscatter node (BN) in this paper) is allowed to modulate its information on the ambient primary radio frequency (RF) signals and to reflect the modulated signals to its associated receivers via varying the intrinsic antenna impedance [6]. However, due to the spectrum sharing and non-cooperation natures between the primary and backscatter links, the IoT device's receiver always suffers from the severe co-channel interference caused by the primary transmission, leading to a reduction to the BN's transmission performance [7]. To tackle this issue, symbiotic radio (SR) has been proposed, where the cooperation between the backscatter and primary links provides an opportunity for the BN's receiver to eliminate the co-channel interference via successive interference cancellation (SIC) technique, significantly improving the BN's transmission performance compared to AmBC [8–10].

There are two setups for SR based on the different symbol durations of information transmitted by the primary user and IoT nodes, which are parasitic SR (PSR) and commensal SR (CSR), respectively [11]. Specifically, for PSR, the symbol duration of the primary user is the same as or comparable to that of the IoT node. In this case, the co-channel interference always affects both the primary transmission and the BN's BackCom [12]. To tackle it, the destination node (DN) employs the SIC to decode the primary information and the backscattered information sequentially. For example, the DN will initially decode the primary information by treating the backscattered signal as interference since the primary signal usually exhibits greater strength compared to the backscattered signal, which undergoes double fading. After successfully decoding the primary information, the DN can subtract the primary signal from the received signal and then decode the backscattered information from the remaining signal. With SIC adopted at the DN, the BN's performance can be significantly improved [13]. For CSR, the symbol duration of the primary user is much smaller than that of the IoT node. In this case, the backscattered link can be regarded as an additional multipath for the primary information to enhance the primary transmission. Accordingly, the joint decoding scheme [14] is employed at the DN to sequentially decode the primary information and the backscattered information, resulting in an improvement for both the primary transmission and the BN's BackCom.

To date, both PSR and CSR have attracted a lot of interests from both academia and industries. Specifically, the authors in [11] derived the closed-form expressions of the outage probabilities for both the primary user and the BN in PSR with imperfect SIC, and then analyzed the corresponding diversity gains. Taking non-orthogonal multiple access (NOMA) into account in PSR, the authors in [15] derived and analyzed the closed-form expressions of the outage probability and the corresponding diversity gain for each link under the Nakagami-m channel fading model. Further, the authors in [16] proposed an opportunistic PSR and an opportunistic CSR to enhance the existing PSR and CSR in terms of the outage probability for each link. Considering a relay assisted PSR network, the authors in [17] analyzed the outage performance for both the primary and backscattered links and then proposed an modified SIC scheme to improve the outage performance in both links.

The resource allocation has also been studied in PSR/CSR. The authors in [9] proposed two transmit beamforming schemes to maximize the weighted sum rate and minimize the transmit power in the single-BN PSR/CSR, respectively. Extending [9] into PSR/CSR with short-packet communication at the BN, the authors in [18] restudied the achievable rate for each transmission in both PSR and CSR and then redesigned the above resource allocation schemes. Considering particular fading state, the authors in [19] analyzed the achievable rates for both the primary and backscatter transmissions and then proposed optimal power allocation schemes for maximize the achievable rate for each transmission in single-BN PSR. Taking the optimization of the power reflection coefficient at the BN into account, the authors in [20] studied the weighted sum-rate maximization in single-BN PSR and CSR, respectively. Further, the authors in [13] extended the work in [20] to multiple-BNs PSR/CSR and then maximized the system energy efficiency (EE) that is defined as the ratio of the total achievable bits to the corresponding energy consumption by jointly optimizing parameters such as the primary transmission power and IoT node reflection coefficient. Combining PSR and CSR in a network, the authors in [10] proposed a cooperative commensal and parasitic scheme for SR and then maximized the achievable primary rate by jointly optimizing the transmit beamforming at the base station. Considering the hardware impairments (HIs) inhere at the transceiver, the authors in [7] theoretically proved that the mutualism relationship between the AmBC and primary links is maintained under HIs and then proposed two schemes to maximize the weighted sum rate for the single-BN and multiple-BNs CSR, respectively. In order to ensure secure communication for the BN while meeting the quality of service (QoS) requirements of the primary link, the authors in [21] maximized the achievable secrecy rate at the BN in the single-BN PSR by jointly optimizing primary transmit beamforming and power sharing between information and artificial noise (AN) signals. Considering a full-duplex single-BN PSR network, the optimum AN power allocation scheme was studied to enhance physical layer. security in [22]. Furthermore, extensive research has been conducted on integrating PSR/CSR with RIS, wherein RIS functions as the BN reflecting its own information to the DN. As for RIS assisted PSR/CSR, different resource allocation schemes have been designed for achieving different optimization goals, that is, the primary system EE maximization [23], the bit error rate minimization [24], the weighted sum-rate maximization [25], and the transmit power minimization [26].

All the above works on PSR/CSR [7, 9, 10, 13, 18–26] have assumed that there exist direct communication links from both the primary transmitter (PT) and the BN to the DN. However, in many practical application scenarios such as industrial automation and smart farm, the direct communication links may not exist due to considerable path attenuation and shadowing effects. Especially, for the backscattered link, it is subject to severer path loss and shadowing due to its susceptibility to double fading. Thus, it is more probable that the direct communication link between the BN and the DN becomes obstructed. To tackle this, relay technology can be leveraged to boost performance for both PT and BN's transmissions. For relay assisted PSR, the system EE stands as a crucial metric while it has not been studied yet, which motivates this work. The main contributions of this work are summarized as follows.

- We maximize the system EE of a relay assisted PSR network, where a decode-and-forward (DF) relay node (RN) is deployed to support both PT and BN's transmissions. We first formulate a problem for maximizing the system EE by jointly optimizing the transmit power of the PT, the power reflection coefficient of the BN, the transmit power and the power allocation ratio at the RN, as well as the SIC decoding order at the DN. As the optimization variable of the SIC decoding order is an integer and several optimization variables are coupled with each other, the formulated problem is non-convex and difficult to solve.

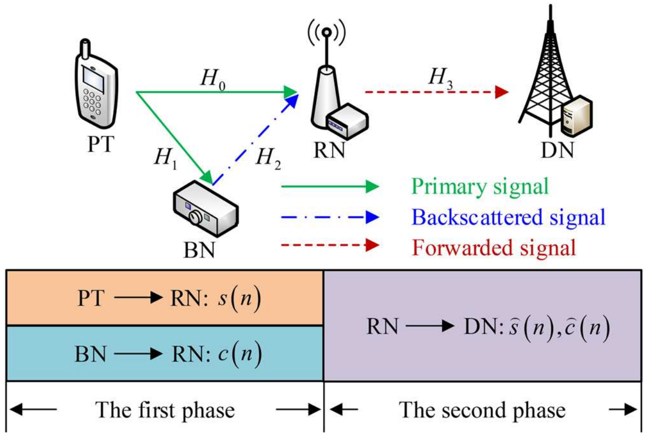

FIGURE 1 | System model.

- To solve this non-convex problem, we decompose it into two subproblems corresponding to the two different decoding orders at the DN. The optimal solution of the subproblem yielding a higher system EE will return a near-optimal solution to the original problem. Accordingly, we develop efficient iterative algorithms to solve the two subproblems. Specifically, for each subproblem, we employ the Dinkelbach-based method to convert the objective function from the fractional form into a more tractable subtraction form and then further divide the converted subproblem into two independent subsubproblems by means of the block coordinate descent (BCD) method. The two sububproblems are proved to be convex and can be solved by using the existing convex tools.
- Simulation results are provided to evaluate the performance of our work. Specifically, the rapid convergence of the proposed iterative algorithms are verified and the superiority of the proposed algorithms in terms of the system EE is demonstrated by comparing with several benchmark schemes.

2 | System Model

As shown in Figure 1, we consider a relay assisted PSR network, which consists of one PT, one BN, one RN and one DN. Assume that all nodes are equipped with a single antenna and work in the half-duplex mode. Following [17, 27], we suppose that the direct communication links between the PT/BN and DN are blocked due to considerable path attenuation and shadowing effects. Therefore, the RN is deployed to support both primary and BN's transmissions. Specifically, the BN modulates its own information on the primary signal and then backscatters the modulated signal to the RN via BackCom. After successfully decoding both primary and backscattered information, the RN forwards the decoded information to the DN. All channels are assumed to undergo quasi-static Rayleigh fading, where the channel gain of each link within each transmission block remains unchanged and may vary among different transmission blocks. Let h_0, h_1, h_2, and h_3 represent the small-scale channel gains of the PT-RN link, the PT-BN link, the BN-RN link, and the RN-DN link, respectively. Denote d_0, d_1, d_2, and d_3 as the distances corresponding to the above links and α_0, α_1, α_2 and α_3 as the corresponding path loss exponents. Following the standard channel model in [17], the channel gains of the PT-RN link, the PT-BN link, the BN-RN link, and the RN-DN link are given by $H_0 = h_0 d_0^{-\alpha_0}$, $H_1 = h_1 d_1^{-\alpha_1}$, $H_2 = h_2 d_2^{-\alpha_2}$ and $H_3 = h_3 d_3^{-\alpha_3}$, respectively. Please note that the information of H_0, H_1, H_2 and H_3 in each transmission block can be obtained at the beginning of the transmission block by using the existing channel estimation methods. Specifically, the information of H_0 and H_3 is estimated via several existing channel estimation methods, for example, least-square estimation, while the information of H_1 and H_2 can be obtained by using the channel estimation method in [28]. On this basis, the system EE maximization based resource allocation scheme can be designed and then applied at each node.

Let T denote the duration of the whole transmission block, which can be equally divided into two phases. In the first phase with duration of $\frac{T}{2}$, the PT transmits its information $s(n), n \in [0, T]$ with the transmit power P_t. Then both the RN and the BN can receive the primary signal. At the BN, it can divide the incident signal into two parts based on its power reflection coefficient β, where one part is used for information backscattering and the other part is harvested to support the energy consumption of the BN's BackCom. Let $\eta \in [0, 1]$ represent the energy conversion efficiency of the energy harvester at the BN [29]. Then the harvested energy at the BN can be computed as

$$E_{\mathrm{BN}} = \frac{T}{2}\eta(1-\beta)P_t H_1. \tag{1}$$

For information backscattering, the BN backscatters its information $c(n), n \in [0, T]$ via BackCom. Then the received signal at the RN can be expressed as

$$y_{\mathrm{RN}}(n) = \sqrt{P_t H_0}s(n) + \sqrt{P_t \beta H_1 H_2}c(n)s(n) + z_{\mathrm{R}}(n), \tag{2}$$

where z_{R} is the additive white Gaussian noise (AWGN) at RN with power σ^2.

In order to decode $s(n)$ and $c(n)$, the BN employs SIC, where $s(n)$ is decoded first by treating $\sqrt{P_t \beta H_1 H_2}c(n)s(n)$ as interference and then $c(n)$ is decoded after removing $\sqrt{P_t H_0}s(n)$ from $y_{\mathrm{RN}}(n)$. Accordingly, the signal to interference plus noise ratio (SINR) for decoding $s(n)$ is given by

$$\gamma_{\mathrm{R},s} = \frac{P_t H_0}{P_t \beta H_1 H_2 + \sigma^2}. \tag{3}$$

When $\gamma_{\mathrm{R},s}$ is not less than its decoding threshold, the RN can successfully decode $s(n)$ and remove $\sqrt{P_t H_0}s(n)$. Accordingly, we can obtain the following inequality to ensure the successful SIC, given by,

$$\gamma_{\mathrm{R},s} \geq \gamma_{\mathrm{th}}^{s} \Leftrightarrow \frac{P_t H_0}{P_t \beta H_1 H_2 + \sigma^2} \geq \gamma_{\mathrm{th}}^{s}, \tag{4}$$

where γ_{th}^{s} denotes the required threshold for decoding $s(n)$. After successfully cancelling $\sqrt{P_t H_0}s(n)$, the signal-to-noise ratio (SNR) for decoding $c(n)$ is expressed as

$$\gamma_{\mathrm{R},c} = \frac{P_t \beta H_1 H_2}{\sigma^2}. \tag{5}$$

In order to ensure that the RN can decode $c(n)$ so that the RN can forward the decoded information to the DN, the following inequality should be met, that is,

$$\gamma_{\mathrm{R},c} \geq \gamma_{\mathrm{th}}^{c} \Leftrightarrow \frac{P_t\beta H_1 H_2}{\sigma^2} \geq \gamma_{\mathrm{th}}^{c}, \tag{6}$$

where γ_{th}^{c} represents the required threshold for decoding $c(n)$.

If both (4) and (6) are satisfied, the RN can decode $s(n)$ and $c(n)$ successfully. Let $\widehat{s}(n)$ and $\widehat{c}(n)$ denote the decoded information at the RN. Then the RN can forward the decoded information to the DN in the second phase. Let P_r denote the transmit power of the RN, which can be divided into two parts based on its power allocation ratio $\rho \in [0, 1]$. Specifically, ρP_r is allocated for forwarding $\widehat{s}(n)$ while $\widehat{c}(n)$ is forwarded with the transmit power $(1-\rho)P_r$. Correspondingly, the signal received at the DN is represented as

$$y_{\mathrm{DN}}(n) = \left(\sqrt{\rho}\,\widehat{s}(n) + \sqrt{1-\rho}\,\widehat{c}(n)\right)\sqrt{P_r H_3} + z_{\mathrm{D}}(n), \tag{7}$$

where z_{D} is the AWGN at the DN with power σ^2.

At the DN, there are two SIC decoding schemes. For the first SIC decoding scheme, the DN first decodes $\widehat{s}(n)$ while considering $\sqrt{(1-\rho)P_r H_3}\,\widehat{c}(n)$ as interference, subsequently decodes $\widehat{c}(n)$ following successful cancellation of $\sqrt{\rho P_r H_3}\,\widehat{s}(n)$. For the second SIC decoding scheme, the DN first decodes $\widehat{c}(n)$ while treating $\sqrt{\rho P_r H_3}\,\widehat{s}(n)$ as interference and proceeds to decode $\widehat{s}(n)$ after eliminating $\sqrt{(1-\rho)P_r H_3}\,\widehat{c}(n)$.

In the first SIC decoding scheme, the SINR for decoding $\widehat{s}(n)$ at the DN is calculated as

$$\gamma_{\mathrm{D},s}^{(1)} = \frac{\rho P_r H_3}{(1-\rho)P_r H_3 + \sigma^2}. \tag{8}$$

If the following inequality is met, then the DN can effectively execute SIC.

$$\gamma_{\mathrm{D},s}^{(1)} \geq \gamma_{\mathrm{th}}^{s} \Leftrightarrow \frac{\rho P_r H_3}{(1-\rho)P_r H_3 + \sigma^2} \geq \gamma_{\mathrm{th}}^{s}. \tag{9}$$

With (9), the SNR for decoding $\widehat{c}(n)$ at the DN is given by

$$\gamma_{\mathrm{D},c}^{(1)} = \frac{(1-\rho)P_r H_3}{\sigma^2}. \tag{10}$$

Based on (10), the successful decoding of $\widehat{c}(n)$ is guaranteed when (11) is satisfied.

$$\gamma_{\mathrm{D},c}^{(1)} \geq \gamma_{\mathrm{th}}^{c} \Leftrightarrow \frac{(1-\rho)P_r H_3}{\sigma^2} \geq \gamma_{\mathrm{th}}^{c}. \tag{11}$$

On this basis, the achievable transmission bits for the primary transmission and BN's BackCom under the first SIC decoding scheme are expressed as

$$R_1^{(1)} = \frac{T}{2}B\log_2\left(1 + \min\left\{\frac{P_t H_0}{P_t\beta H_1 H_2 + \sigma^2}, \frac{\rho P_r H_3}{(1-\rho)P_r H_3 + \sigma^2}\right\}\right), \tag{12}$$

$$R_2^{(1)} = \frac{T}{2}B\log_2\left(1 + \min\left\{\frac{P_t\beta H_1 H_2}{\sigma^2}, \frac{(1-\rho)P_r H_3}{\sigma^2}\right\}\right), \tag{13}$$

In the second SIC decoding scheme, the SINR for decoding $\widehat{c}(n)$ can be determined by

$$\gamma_{\mathrm{D},c}^{(2)} = \frac{(1-\rho)P_r H_3}{\rho P_r H_3 + \sigma^2}. \tag{14}$$

Similar to (4), the following equality must be fulfilled to ensure successful SIC at the DN.

$$\gamma_{\mathrm{D},c}^{(2)} \geq \gamma_{\mathrm{th}}^{c} \Leftrightarrow \frac{(1-\rho)P_r H_3}{\rho P_r H_3 + \sigma^2} \geq \gamma_{\mathrm{th}}^{c}. \tag{15}$$

With (15), the SNR for decoding $\widehat{s}(n)$ is given by

$$\gamma_{\mathrm{D},s}^{(2)} = \frac{\rho P_r H_3}{\sigma^2}. \tag{16}$$

Similar to (9), we have

$$\gamma_{\mathrm{D},s}^{(2)} \geq \gamma_{\mathrm{th}}^{s} \Leftrightarrow \frac{\rho P_r H_3}{\sigma^2} \geq \gamma_{\mathrm{th}}^{s}. \tag{17}$$

Accordingly, the achievable transmission bits of the primary transmission and BN's BackCom under the second SIC decoding scheme can be expressed as

$$R_1^{(2)} = \frac{T}{2}B\log_2\left(1 + \min\left\{\frac{P_t H_0}{P_t\beta H_1 H_2 + \sigma^2}, \frac{\rho P_r H_3}{\sigma^2}\right\}\right), \tag{18}$$

$$R_2^{(2)} = \frac{T}{2}B\log_2\left(1 + \min\left\{\frac{P_t\beta H_1 H_2}{\sigma^2}, \frac{(1-\rho)P_r H_3}{\rho P_r H_3 + \sigma^2}\right\}\right). \tag{19}$$

Let $a \in \{0, 1\}$ decide which SIC decoding scheme is employed at the DN. Specifically, when $a = 0$, the DN uses the first SIC decoding scheme to decode $\widehat{s}(n)$ and $\widehat{c}(n)$. When $a = 1$, the second SIC decoding scheme is considered at the DN. Accordingly, the achievable transmission bits of the primary transmission and BN's BackCom are determined by

$$R_1 = (1-a)R_1^{(1)} + aR_1^{(2)}, \tag{20}$$

$$R_2 = (1-a)R_2^{(1)} + aR_2^{(2)}, \tag{21}$$

Likewise, the decoding SINR/SNR at the DN for decoding $\widehat{s}(n)$ and $\widehat{c}(n)$ are written as

$$\gamma_{\mathrm{D},s} = (1-a)\gamma_{\mathrm{D},s}^{(1)} + a\gamma_{\mathrm{D},s}^{(2)}, \tag{22}$$

$$\gamma_{\mathrm{D},c} = (1-a)\gamma_{\mathrm{D},c}^{(1)} + a\gamma_{\mathrm{D},c}^{(2)}. \tag{23}$$

3 | System EE Maximization

In this section, we present an optimization problem aiming at maximizing the system EE of the considered network. This is achieved through the joint optimization of the transmit power of the PT P_t, the transmit power P_r and the power allocation ratio ρ at the RN, the power reflection coefficient of the BN β and the factor of the SIC decoding order at the DN a. Given that the formulated problem is non-convex and computationally challenging, we propose iterative algorithms utilizing Dinkelbach's method and the BCD method for solution.

3.1 | Problem Formulation

The objective function of the optimization problem is the system EE. which is defined as the ratio of the system transmission bits and the total energy consumption of the whole network. For the system transmission bits, we consider the weighted sum transmission bits achieved by the primary transmission and BN's BackCom. Let w_1 and w_2 represent the weights of the primary and backscattered links, respectively, which indicates the priority of the primary and backscattered links. Then the weighted sum transmission bits can be expressed as $w_1R_1 + w_2R_2$. For the total energy consumption, it can be computed as $(P_t + P_s + P_r + P_{\mathrm{R},s})\frac{T}{2}$, where P_s and $P_{\mathrm{R},s}$ represent the constant circuit power consumption at the PT and the RN, respectively. Correspondingly, the system EE can be determined by $\frac{w_1R_1+w_2R_2}{(P_t+P_s+P_r+P_{\mathrm{R},s})\frac{T}{2}}$.

Let P_c denote the circuit power consumption of BackCom at the BN. Following [17], the energy consumption at the BN for BackCom is given by $P_c\frac{T}{2}$.

Accordingly, the system EE maximization problem can be formulated as

$$\begin{aligned}
&\max_{\beta,\rho,P_t,P_r,a} \frac{w_1R_1 + w_2R_2}{(P_t + P_s + P_r + P_{\mathrm{R},s})\frac{T}{2}} \\
&\text{s.t.C1} : R_1 \geq R_{P,\min}, \\
&\quad \text{C2} : R_2 \geq R_{B,\min}, \\
&\quad \text{C3} : \gamma_{\mathrm{R},s} \geq \gamma^s_{\mathrm{th}}, \gamma_{\mathrm{R},c} \geq \gamma^c_{\mathrm{th}}, \gamma_{\mathrm{D},s} \geq \gamma^s_{\mathrm{th}}, \gamma_{\mathrm{D},c} \geq \gamma^c_{\mathrm{th}}, \\
&\quad \text{C4} : \frac{T}{2}\eta(1-\beta)P_tH_1 \geq P_c\frac{T}{2}, \\
&\quad \text{C5} : 0 \leq P_t \leq P_{t,\max}, 0 \leq P_r \leq P_{r,\max}, \\
&\quad \text{C6} : 0 \leq \beta \leq 1, 0 \leq \rho \leq 1, a \in \{0,1\},
\end{aligned} \tag{24}$$

where $R_{P,\min}$ and $R_{B,\min}$ are the minimum required transmission bits of the primary and backscattered links; $P_{t,\max}$ and $P_{r,\max}$ represent the maximum allowed transmission power at the PT and the RN, respectively.

In the above problem, C1 and C2 are the quality of service (QoS) constraints for the primary transmission and BN's BackCom. In particular, the achievable transmission bits for the primary transmission or BN's BackCom should not be less than its minimum required transmission bits. C3 ensures that $s(n)$, $c(n)$, $\frown{s}(n)$ and $\frown{c}(n)$ are successfully decoded at the RN and the DN, respectively. C4 is the energy-causality constraint for the BN, which guarantees that the energy consumption of BackCom at the BN should not be larger than its harvested energy so that the BN can successfully BackCom. C5 is the constraint that constrains the maximum transmit power for both the PT and the RN. C6 provides the ranges of the power reflection coefficient of the BN β, the power allocation ratio of the RN ρ and the factor of the SIC decoding order at the DN a.

By observation, we find that the formulated problem is a highly non-convex mixed-integer programming problem due to the following three aspects. First, the objective function includes the complicate fractional form, leading to multiple coupled relationships among multiple optimization variables. Second, the discrete nature of SIC decoding order brings the integer optimization, resulting in a mixed-integer optimization problem. Third, several coupled relationships among multiple optimization variables exist due to the co-channel interference between the primary transmission and BN's BackCom, the complex objective function, etc.

3.2 | Solution and Algorithms

This subsection is provided to tackle this non-convex problem. First, to deal with the integer optimization, we decouple the formulated problem into two distinct problems based on different values of a. Specifically, with $a = 0$, the optimization problem (24) can be transformed as

$$\begin{aligned}
&\max_{\beta,\rho,P_t,P_r} \frac{w_1R_1^{(1)} + w_2R_2^{(1)}}{(P_t + P_s + P_r + P_{\mathrm{R},s})\frac{T}{2}} \\
&\text{s.t.C1}-1\text{a} : R_1^{(1)} \geq R_{P,\min}, \\
&\quad \text{C2}-1\text{a} : R_2^{(2)} \geq R_{B,\min}, \\
&\quad \text{C3}-1\text{a} : \gamma_{\mathrm{R},s} \geq \gamma^s_{\mathrm{th}}, \gamma_{\mathrm{R},c} \geq \gamma^c_{\mathrm{th}}, \gamma^{(1)}_{\mathrm{D},s} \geq \gamma^s_{\mathrm{th}}, \gamma^{(1)}_{\mathrm{D},c} \geq \gamma^c_{\mathrm{th}}, \\
&\quad \text{C4, C5, C6}.
\end{aligned} \tag{25}$$

When $a = 1$ holds, we have

$$\begin{aligned}
&\max_{\beta,\rho,P_t,P_r} \frac{w_1R_1^{(2)} + w_2R_2^{(2)}}{(P_t + P_s + P_r + P_{\mathrm{R},s})\frac{T}{2}} \\
&\text{s.t.C1}-1\text{b} : R_1^{(1)} \geq R_{P,\min}, \\
&\quad \text{C2}-1\text{b} : R_2^{(2)} \geq R_{B,\min}, \\
&\quad \text{C3}-1\text{b} : \gamma_{\mathrm{R},s} \geq \gamma^s_{\mathrm{th}}, \gamma_{\mathrm{R},c} \geq \gamma^c_{\mathrm{th}}, \gamma^{(2)}_{\mathrm{D},s} \geq \gamma^s_{\mathrm{th}}, \gamma^{(2)}_{\mathrm{D},c} \geq \gamma^c_{\mathrm{th}}, \\
&\quad \text{C4, C5, C6}.
\end{aligned} \tag{26}$$

After solving (25) and (26) and obtaining their solutions, the solution to the original problem (24) corresponds to that of (25) or (26) with higher system EE. It can be observed that (25) and (26) have similar objective function and constraints. Thus, the methods that are used to solve (25) can also be used to tackle (26). In the following, we are devoted to tackling (25).

Specifically, to address the min function problem in $R_1^{(1)}$ and $R_2^{(1)}$, we introduce two auxiliary variables, denoted by λ_1 and λ_2, to represent $\min\{\frac{P_tH_0}{P_t\beta H_1H_2+\sigma^2}, \frac{\rho P_rH_3}{(1-\rho)P_rH_3+\sigma^2}\}$ and $\min\{\frac{P_t\beta H_1H_2}{\sigma^2}, \frac{(1-\rho)P_rH_3}{\sigma^2}\}$ in $R_1^{(1)}$ and $R_2^{(1)}$, respectively. Specifically, optimization problem

(25) can be rewritten as

$$
\begin{aligned}
&\max_{\beta,\rho,P_t,P_r,\lambda_1,\lambda_2} \frac{w_1\frac{T}{2}B\log_2(1+\lambda_1)+w_2\frac{T}{2}B\log_2(1+\lambda_2)}{(P_t+P_s+P_r+P_{\mathrm{R,s}})\frac{T}{2}}\\
&\text{s.t.C1}-2\text{a}: \frac{T}{2}B\log_2(1+\lambda_1)\ge R_{P,\min},\\
&\quad \text{C2}-2\text{a}: \frac{T}{2}B\log_2(1+\lambda_2)\ge R_{B,\min},\\
&\quad \text{C3}-1\text{a}, \text{C4}, \text{C5}, \text{C6},\\
&\quad \text{C7}: \frac{P_tH_0}{P_t\beta H_1H_2+\sigma^2}\ge\lambda_1,\\
&\quad \text{C8}: \frac{\rho P_rH_3}{(1-\rho)P_rH_3+\sigma^2}\ge\lambda_1,\\
&\quad \text{C9}: \frac{P_t\beta H_1H_2}{\sigma^2}\ge\lambda_2,\\
&\quad \text{C10}: \frac{(1-\rho)P_rH_3}{\sigma^2}\ge\lambda_2.
\end{aligned}
\tag{27}
$$

It can be observed that problem (27) is still non-convex due to the complex objective function in a fractional form and several coupling relationships. To address the fractional form in the objective function, we transform the objective function from a fractional form into a subtractive form by means of the Dinkelbach's method [30]. Specifically, denote the maximum system EE of the considered network as q^*. Then the following lemma is provided to determine q^*.

Lemma 1. *According to the Dinkelbach's method, the optimal solution to problem (27) can be achieved only when the following equation (28) holds.*

$$
\begin{aligned}
&\max_{\beta,\rho,P_t,P_r,\lambda_1,\lambda_2} w_1B\log_2(1+\lambda_1)+w_2B\log_2(1+\lambda_2)\\
&-q^*\left(P_t+P_s+P_r+P_{\mathrm{R,s}}\right)\\
&=w_1B\log(1+\lambda_1^*)+w_2B\log(1+\lambda_2^*)\\
&-q^*\left(P_t^*+P_s+P_r^*+P_{\mathrm{R,s}}\right)=0,
\end{aligned}
\tag{28}
$$

where $*$ denotes the optimal solution corresponding to the optimization variable.

Proof. (28) can be proved based on the generalized fractional programming theory. Note that the similar proof can be found in [30] and thus omitted here for brevity. □

Based on (28), we can develop a Dinkelbach-based iterative algorithm to tackle problem (27) and the detailed process is shown in Algorithm 1. In particular, let $l\,(l\ge 1)$ denote the number of iterations for Algorithm 1 and initialize the value of q to 0. Subsequently, in the l-th iteration, we address problem (29) under a given parameter q and obtain the corresponding solution, denoted as $\{\beta^l,\rho^l,P_t^l,P_r^l,\lambda_1^l,\lambda_2^l\}$. Then we can compute the system EE of this network utilizing the obtained solution in this iteration, denoted as q_l, given by $q_l=\frac{w_1B\log_2(1+\lambda_1^l)+w_2B\log_2(1+\lambda_2^l)}{P_t^l+P_s+P_r^l+P_{\mathrm{R,s}}}$. Let ε_D denote the maximum error tolerance of Algorithm 1. When q_l satisfies the stopping condition, that is, $|q_l-q|<\varepsilon_D$, then we have $q^*=q_l$ and output the solution obtained in this iteration as the optimal solution to problem (27), namely $\{\beta^*,\rho^*,P_t^*,P_r^*,\lambda_1^*,\lambda_2^*\}=\{\beta^l,\rho^l,P_t^l,P_r^l,\lambda_1^l,\lambda_2^l\}$. Otherwise, we should update q as q_l and repeat the above steps until the stopping condition is met.

ALGORITHM 1 | Dinkelbach-Based Iterative Algorithm for Solving (27).

Initialize the maximum number of iterations $L_{\max}$, and the maximum error tolerance ε_D;
Set $q=0$ and $l=1$;
repeat
  Solve problem (29) under a given q, and obtain its optimal solution, denoted by $\{\beta^l,\rho^l,P_t^l,P_r^l,\lambda_1^l,\lambda_2^l\}$;
  Compute the system EE of this network q_l as $q_l=\frac{w_1B\log_2(1+\lambda_1^l)+w_2B\log_2(1+\lambda_2^l)}{P_t^l+P_s+P_r^l+P_{\mathrm{R,s}}}$;
  if $|q_l-q|<\varepsilon_D$ holds **then**
    Set $q^*=q_l$ and $\{\beta^*,\rho^*,P_t^*,P_r^*,\lambda_1^*,\lambda_2^*\}=\{\beta^l,\rho^l,P_t^l,P_r^l,\lambda_1^l,\lambda_2^l\}$;
    Set Flag $=1$ and return;
  else
    Set $q=q_l$, $l=l+1$, and Flag $=0$;
  end if
until Flag $=1$ or $l=L_{\max}$.

Based on Algorithm 1, we find the main challenge for solving problem (27) is to solve problem (29), which is given by

$$
\begin{aligned}
&\max_{\beta,\rho,P_t,P_r,\lambda_1,\lambda_2} w_1B\log_2(1+\lambda_1)+w_2B\log_2(1+\lambda_2)\\
&-q\left(P_t+P_s+P_r+P_{\mathrm{R,s}}\right)\\
&\text{s.t.C1}-2\text{a}, \text{C2}-2\text{a}, \text{C3}-1\text{a}, \text{C4}-\text{C10}.
\end{aligned}
\tag{29}
$$

However, problem (29) is still non-convex due to the coupled relationships. In order to handle the coupled relationships between P_t and β, and between P_r and ρ, we introduce three auxiliary variables, denoted by x, P_1 and P_2, to replace β, ρ, and P_r in problem (29), where $x=P_t\beta$, $P_1=\rho P_r$, and $P_2=(1-\rho)P_r$. Then problem (29) can be reformulated as

$$
\begin{aligned}
&\max_{x,P_1,P_t,P_2,\lambda_1,\lambda_2} w_1B\log_2(1+\lambda_1)+w_2B\log_2(1+\lambda_2)\\
&-q\left(P_t+P_s+P_1+P_2+P_{\mathrm{R,s}}\right)\\
&\text{s.t.C1}-2\text{a}, \text{C2}-2\text{a},\\
&\quad \text{C3}-2\text{a}: \frac{P_tH_0}{xH_1H_2+\sigma^2}\ge\gamma_{\mathrm{th}}^s, \frac{xH_1H_2}{\sigma^2}\ge\gamma_{\mathrm{th}}^c,\\
&\qquad \frac{P_1H_3}{P_2H_3+\sigma^2}\ge\gamma_{\mathrm{th}}^s, \frac{P_2H_3}{\sigma^2}\ge\gamma_{\mathrm{th}}^c,\\
&\quad \text{C4}-1\text{a}: \eta(P_t-x)H_1\ge P_c,\\
&\quad \text{C5}-1\text{a}: 0\le P_t\le P_{t,\max}, 0\le P_1+P_2\le P_{r,\max},
\end{aligned}
$$

$$\mathrm{C6-1a}: 0 \le x \le P_t, 0 \le P_1 \le P_1 + P_2,$$

$$\mathrm{C7-1a}: \frac{P_t H_0}{x H_1 H_2 + \sigma^2} \ge \lambda_1,$$

$$\mathrm{C8-1a}: \frac{P_1 H_3}{P_2 H_3 + \sigma^2} \ge \lambda_1,$$

$$\mathrm{C9-1a}: \frac{x H_1 H_2}{\sigma^2} \ge \lambda_2,$$

$$\mathrm{C10-1a}: \frac{P_2 H_3}{\sigma^2} \ge \lambda_2. \tag{30}$$

As for problem (30), the objective function is concave and constraints $\mathrm{C1-2a}$, $\mathrm{C2-2a}$, $\mathrm{C4-1a}$, $\mathrm{C5-1a}$ and $\mathrm{C6-1a}$ are convex. As for $\mathrm{C3-2a}$, it can be transformed into linear constraints, that is,

$$\begin{aligned}\mathrm{C3-3a}: & P_t H_0 \ge \gamma_{\mathrm{th}}^{s}\left(x H_1 H_2 + \sigma^2\right), x H_1 H_2 \ge \gamma_{\mathrm{th}}^{c} \sigma^2, \\ & P_1 H_3 \ge \gamma_{\mathrm{th}}^{s}\left(P_2 H_3 + \sigma^2\right), P_2 H_3 \ge \gamma_{\mathrm{th}}^{c} \sigma^2.\end{aligned} \tag{31}$$

Therefore, the main non-convexity of problem (30) is caused by the non-convexity of $\mathrm{C7-1a}$, $\mathrm{C8-1a}$, $\mathrm{C9-1a}$ and $\mathrm{C10-1a}$. To address it, we use the BCD method to decouple (30) into two subproblems, which are the subproblem under a given x and P_2 and the subproblem under a given P_1, P_t, λ_1 and λ_2.

Specifically, with a given x and P_2, problem (30) can be transformed as

$$\begin{aligned}\max_{P_1, P_t, \lambda_1, \lambda_2} \; & w_1 B \log_2(1+\lambda_1) + w_2 B \log_2(1+\lambda_2) \\ & - q\left(P_t + P_s + P_1 + P_2 + P_{\mathrm{R,s}}\right) \\ \mathrm{s.t.} \; & \mathrm{C1-2a, C2-2a, C3-3a, C4-1a, C5-1a,} \\ & \mathrm{C6-1a, C7-1a, C8-1a, C9-1a, C10-1a.}\end{aligned} \tag{32}$$

In problem (32), $\mathrm{C7-1a}$, $\mathrm{C8-1a}$, $\mathrm{C9-1a}$ and $\mathrm{C10-1a}$ are linear constraints with respect to P_1, P_t, λ_1 and λ_2. Therefore, (32) is a convex problem, which can be optimally solved by using the existing standard convex optimization tools, that is, the interior point method [31], etc.

With a given P_1, P_t, λ_1 and λ_2, problem (30) can be reformulated as

$$\begin{aligned}\max_{x, P_2} \; & w_1 B \log_2(1+\lambda_1) + w_2 B \log_2(1+\lambda_2) \\ & - q\left(P_t + P_s + P_1 + P_2 + P_{\mathrm{R,s}}\right) \\ \mathrm{s.t.} \; & \mathrm{C3-3a, C4-1a, C5-1a, C6-1a,} \\ & \mathrm{C7-2a}: P_t H_0 \ge \lambda_1\left(x H_1 H_2 + \sigma^2\right), \\ & \mathrm{C8-2a}: P_1 H_3 \ge \lambda_1\left(P_2 H_3 + \sigma^2\right), \mathrm{C9-1a, C10-1a.}\end{aligned} \tag{33}$$

It can be observed that constraints $\mathrm{C7-2a}$, $\mathrm{C8-2a}$, $\mathrm{C9-1a}$ and $\mathrm{C10-1a}$ are linear with respect to x and P_2. Thus, problem (33) is proved to be convex and can be solved by using the existing standard convex optimization tools.

Drawing from the preceding analysis, we devise a BCD-based iterative algorithm to address problem (30). The intricate procedure is elucidated in Algorithm 2. Specifically, we initialize x and P_2. Then, in the i-th iteration where $i \ge 1$, we solve subproblem (32) given x and P_2, obtaining its optimal solution denoted as $\{P_1^+, P_t^+, \lambda_1^+, \lambda_2^+\}$. Subsequently, we compute the objective function of subproblem (32), denoted as $E_i^{(1)}$, as follows: $E_i^{(1)} = w_1 B \log_2(1+\lambda_1^+) + w_2 B \log_2(1+\lambda_2^+) - q(P_t^+ + P_s + P_1^+ + P_2 + P_{\mathrm{R,s}})$. Next, we solve subproblem (33) with $P_1 = P_1^+$, $P_t = P_t^+$, $\lambda_1 = \lambda_1^+$, and $\lambda_2 = \lambda_2^+$, obtaining its optimal solution denoted as $\{x^+, P_2^+\}$. Subsequently, we compute the objective function of subproblem (33), denoted as $E_i^{(2)}$, as follows: $E_i^{(2)} = w_1 B \log_2(1+\lambda_1^+) + w_2 B \log_2(1+\lambda_2^+) - q(P_t^+ + P_s + P_1^+ + P_2^+ + P_{\mathrm{R,s}})$. If the stopping condition, namely $\left|E_i^{(1)} - E_i^{(2)}\right| < \varepsilon_B$, is satisfied, we output the solution to problem (30) as $\{x^+, P_1^+, P_t^+, P_2^+, \lambda_1^+, \lambda_2^+\}$, where ε_B denotes the maximum error tolerance of Algorithm 2. Otherwise, we update x and P_2 as $x = x^+$ and $P_2 = P_2^+$, and repeat the preceding steps until the stopping condition is met.

ALGORITHM 2 | BCD-Based Iterative Algorithm for Solving (30).

```
Set i = 1 and initialize x, P_2, the maximum error
tolerance ε_B and the maximum allowed number of
iterations I_max;
repeat
    Solve subproblem (32) under given x and P_2, and
    obtain its optimal solution, denoted by
    {P_1^+, P_t^+, λ_1^+, λ_2^+};
    Compute the objective function of subproblem (32)
    E_i^(1) as E_i^(1) = w_1 B log_2(1 + λ_1^+) + w_2 B log_2(1 + λ_2^+) −
    q(P_t^+ + P_s + P_1^+ + P_2 + P_R,s);
    Solve subproblem (33) with P_1 = P_1^+, P_t = P_t^+, λ_1 = λ_1^+
    and λ_2 = λ_2^+, and obtain its optimal solution, denoted
    by {x^+, P_2^+};
    Compute the objective function of subproblem (33)
    E_i^(2) as E_i^(2) = w_1 B log_2(1 + λ_1^+) + w_2 B log_2(1 + λ_2^+) −
    q(P_t^+ + P_s + P_1^+ + P_2^+ + P_R,s);
    if |E_i^(1) − E_i^(2)| < ε_B then
        Output the solution to (30) as
        {x^+, P_1^+, P_t^+, P_2^+, λ_1^+, λ_2^+};
        Set Flag = 1 and return;
    else
        Set x = x^+ and P_2 = P_2^+;
        Set i = i + 1, and Flag = 0;
    end if
until Flag = 1 or i = I_max.
```

By employing Algorithm 1 and Algorithm 2, we can effectively address problem (27). Specifically, Algorithm 1 is utilized to tackle (27), and within each iteration of Algorithm 1, Algorithm 2 is invoked to solve problem (30), which is derived from (27). Consequently, problem (25) can be resolved. Similarly, by employing a combination of Algorithm 1 and Algorithm 2 with appropriate adjustments, we can also tackle (27). With solutions obtained for both (25) and (27), we can derive a solution for (24).

Then the computational complexity of the proposed algorithm is analyzed as follows. According to [31], the computational complexities for solving (32) and (33) are given by $O(\sqrt{15}\log(15))$ and $O(\sqrt{13}\log(13))$, where $O(\cdot)$ is the big-O notation. Let M_1 and M_2 denote the number of iterations for Algorithm 1 and Algorithm 2, respectively. Then the computational complexity of the proposed algorithm is given by $M_1M_2(O(\sqrt{15}\log(15)) + O(\sqrt{13}\log(13)))$.

4 | Simulation Results

In this section, we discuss the performance of the proposed scheme via computer simulations. Unless otherwise specified, the basic simulation parameters are set as follows. Specifically, we set $T = 4\,\mathrm{s}$, $B = 100\,\mathrm{kHz}$, $\sigma^2 = -80\,\mathrm{dBm}$, $\eta = 0.7$, $\alpha_1 = \alpha_2 = \alpha_3 = 2.7$, $\alpha_4 = 4$, $\gamma_{\mathrm{th}}^{s} = 3$, $\gamma_{\mathrm{th}}^{c} = 0.15$, $W_1 = 0.1$, $W_2 = 0.9$, $P_s = P_{\mathrm{R},s} = 1\,\mathrm{mW}$, $R_{\mathrm{P,min}}$=100 kbits, $\mathrm{R}_{\mathrm{B,min}} = 10$ kbits, $P_{t,\max} = 30$ dBm, $P_{r,\max} = 10$ mW, $P_c = 8.9\ \mu\mathrm{W}$, $d_0 = 25$ m, $d_1 = 5$ m, $d_2 = 24$ m, and $d_3 = 200$ m.

Figure 2 is provided to show the convergence of Algorithm 1 under varying settings of $R_{P,\min}$, specifically at 100 kbits, 110 kbits and 120 kbits, respectively. Figure 2a demonstrates the convergence under the first SIC decoding scheme, while Figure 2b depicts the convergence under the second SIC decoding scheme. It is evident that Algorithm 1 achieves convergence after 8/7 iterations under the first/second SIC decoding scheme, indicating its rapid convergence rate. Moreover, it is noticeable that the system EE decreases under both schemes as $R_{P,\min}$ increases. This trend is attributed to the stricter nature of constraint C1 with larger $R_{P,\min}$. Consequently, more resources are allocated to primary transmission to adhere to this constraint, leading to a reduction in system EE.

Figure 3 depicts the convergence of Algorithm 2 under both the first and second SIC decoding schemes. In this figure, subproblem 1 refers to problem (32) with fixed values for both x and P_2, while subproblem 2 corresponds to problem (33) with given P_1, P_t, λ_1, and λ_2. Observing the convergence under different decoding schemes, it is evident that the system EE under subproblem 1 consistently converges to the same value as that under subproblem 2 after only 3 iterations. This illustrates the rapid convergence rate of Algorithm 2.

In order to demonstrate the advantages of the proposed scheme, we conduct a comparative analysis of the system EE between the proposed scheme and the following three baseline schemes, namely the random SIC decoding scheme, the worst-case SIC decoding scheme and relay-assisted wireless powered cognitive radio, respectively.

- **The Random SIC Decoding Scheme**: In this scheme, the DN randomly selects between the first and second SIC decoding schemes. With a chosen SIC decoding scheme, the variables β, ρ, P_t and P_r are jointly optimized to maximize the system EE using the proposed efficient algorithms. For instance, if the first SIC decoding scheme is selected, we employ the proposed efficient algorithms to solve problem (25). Conversely, if the second SIC decoding scheme is cho-

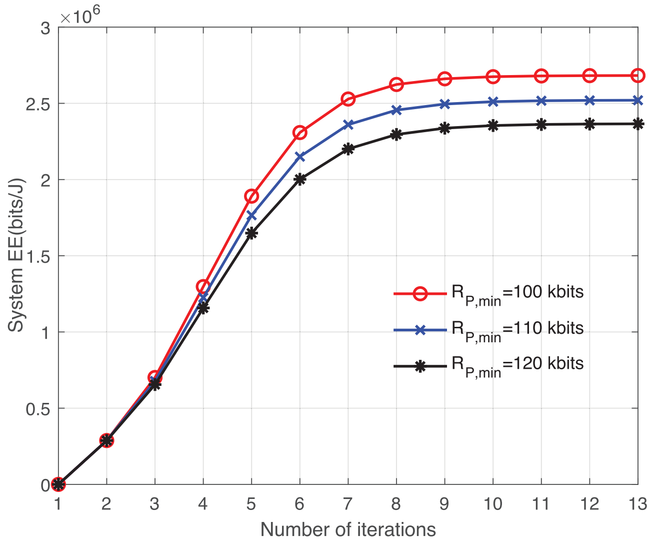

(a) The first SIC decoding scheme.

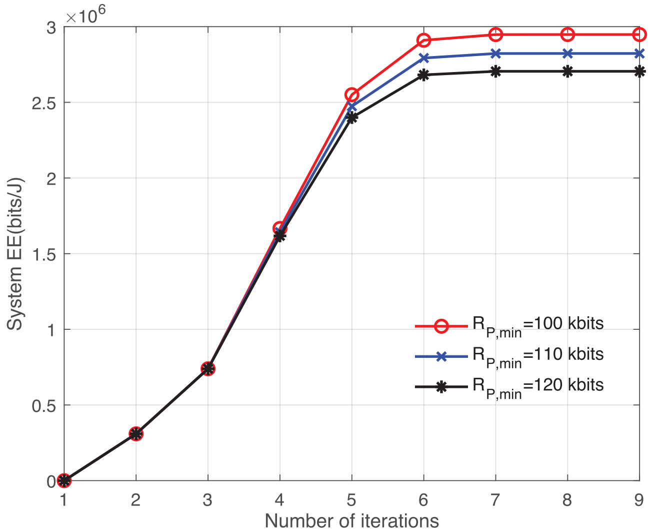

(b) The second SIC decoding scheme.

FIGURE 2 | The convergence of Algorithm 1.

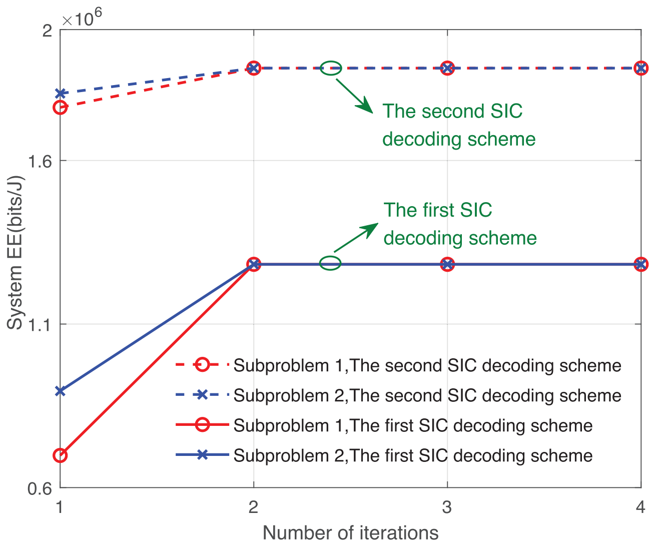

FIGURE 3 | The convergence of Algorithm 2.

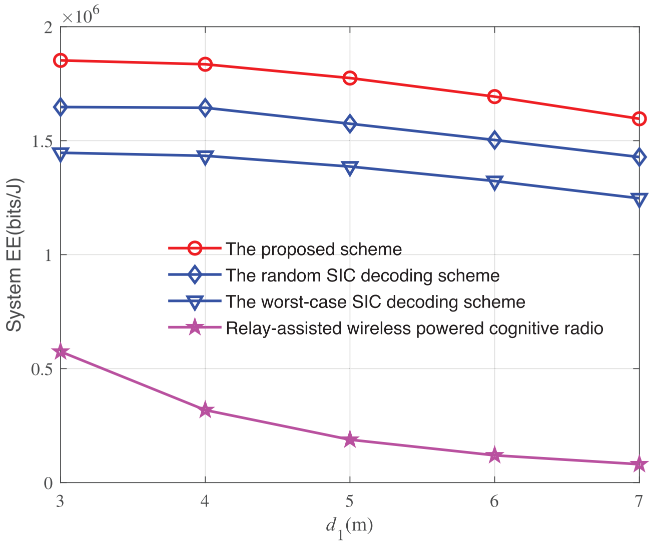

FIGURE 4 | The system EE of the considered network versus the distance between the PT and the BN.

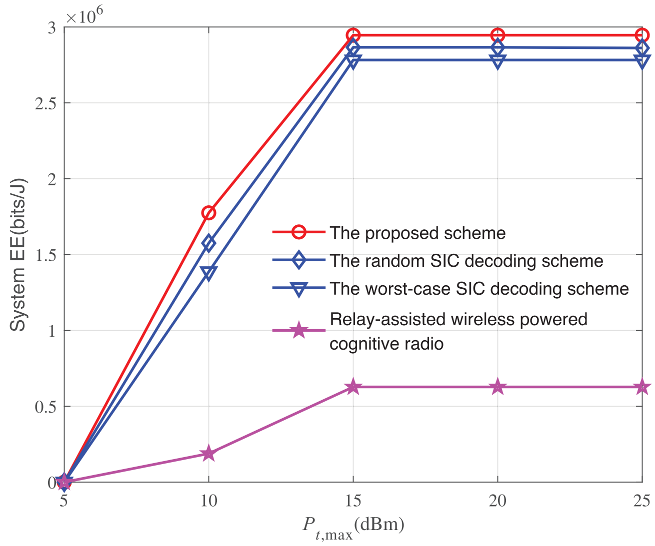

FIGURE 5 | The system EE of the considered network versus the maximum allowed transmission power at the PT.

sen, problem (26) is addressed using the proposed efficient algorithms.

- **The Worst-Case SIC Decoding Scheme**: This scheme corresponds to the solution obtained from either problem (25) or problem (26), whichever yields a lower system EE. Similarly, the implementation of this scheme is facilitated by employing the proposed efficient algorithms.
- **Relay-Assisted Wireless Powered Cognitive Radio**: In this scheme, the BN transmits its information $c(n)$ to the RN through active communication, rather than utilizing BackCom. Consequently, the variables a, ρ, P_t and P_r along with the transmit power of the BN are collectively optimized to maximize the system EE. To realize this objective, the methodologies employed in this work are still applicable with some necessary modifications.

Figure 4 illustrates the system EE of the considered network as a function of the distance between the PT and the BN d_1. In order to demonstrate the superiority of the proposed scheme, we compare the system EE of the considered network under the proposed scheme with that under the random SIC decoding scheme, the worst-case SIC decoding scheme and relay-assisted wireless powered cognitive radio. It can be observed that as d_1 increases, there is a discernible decrease in the system EE across all schemes. This phenomenon arises from the weakened signal received at the BN with larger d_1, resulting in diminished harvested energy and attenuated signal backscattering at the BN. Consequently, to adhere to the energy-causality and QoS constraints at the BN, more resources are allocated to enhance the BN's performance, thereby reducing the system EE. Furthermore, compared to the three baseline schemes, our proposed scheme consistently achieves the highest system EE, underscoring its superiority in this regard. In particular, the proposed scheme outperforms the random SIC decoding scheme and the worst-case SIC decoding scheme. This superiority stems from the optimization of the SIC decoding order considered at the DN so that the DN always selects the optimal decoding order to achieve the maximum system EE. In comparison to relay-assisted wireless powered cognitive radio, our proposed scheme demonstrates superior EE performance by employing the more energy-efficient communication paradigm, namely BackCom.

Figure 5 shows the system EE of the considered network versus the maximum allowed transmission power at the PT $P_{t,\max}$, where the proposed scheme, the random SIC decoding scheme, the worst-case SIC decoding scheme and relay-assisted wireless powered cognitive radio are employed. As $P_{t,\max}$ increases, it is evident that the system EE initially rises and eventually reaches a convergent state when $P_{t,\max}$ becomes sufficiently large. This behavior can be attributed to the following reasons. When $P_{t,\max}$ is small, the increase of $P_{t,\max}$ results in higher transmission bits which predominantly influence the system EE. Consequently, the system EE increases with the improvement of $P_{t,\max}$. However, as $P_{t,\max}$ becomes sufficiently large, the optimal value of P_t is no longer influenced by $P_{t,\max}$, leading to a stable system EE. Besides, by comparison, we also observe that the proposed scheme outperforms the other schemes in terms of the system EE, demonstrating the superiority of the proposed scheme in this regard.

Figure 6 depicts the system EE of the considered network across the four schemes against the minimum required transmission bits for the primary transmission $R_{P,\min}$, where $R_{P,\min}$ ranges from 100 kbits to 120 kbits. Upon observation, it is evident that the system EE remains unchanged under the proposed scheme, the random SIC decoding scheme, and the worst-case SIC decoding scheme with smaller values of $R_{P,\min}$, and then declines as $R_{P,\min}$ exceeds a certain threshold. Conversely, the system EE under relay-assisted wireless powered cognitive radio consistently diminishes as $R_{P,\min}$ increases. The reasons are as follows. For the proposed scheme, the random SIC decoding scheme and the worst-case SIC decoding scheme, when $R_{P,\min}$ is small, the QoS constraint for the primary transmission is relatively lenient, exerting minimal influence on the optimization variables, thereby maintaining an unchanged system EE. However, as $R_{P,\min}$ increases, the optimization variables become constrained by this QoS requirement. Specifically, a higher $R_{P,\min}$ imposes a stricter constraint,

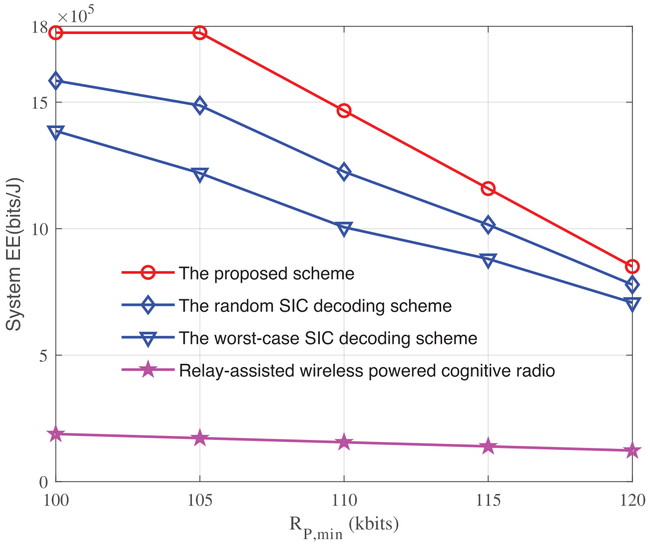

FIGURE 6 | The system EE of the considered network versus the minimum required transmission bits for the primary transmission $R_{P,\min}$.

prompting a reallocation of resources to comply with it, consequently leading to a reduction in system EE. In the case of relay-assisted wireless powered cognitive radio, the transmission bits for the primary transmission are lower compared to the other schemes due to the substantial co-channel interference stemming from the BN's active communication. Consequently, its system EE is affected by $R_{P,\min}$ even when it is relatively small. Moreover, through comparative analysis, it is apparent that the proposed scheme consistently achieves the highest system EE, underscoring its advantage in this regard.

5 | Conclusions

In this work, we have maximized the system EE for the DF relay-assisted parasitic SR network. Specifically, we have formulated the system EE maximization problem for the considered network by jointly optimizing multiple optimization variables, including the transmit power of the PT, the power reflection coefficient of the BN, the transmit power and the power allocation ratio at the RN as well as the SIC decoding order at the DN. Given the highly non-convex nature of the formulated problem, we have employed various optimization techniques such as the Dinkelbach-based method and the BCD method to address it. In particular, we initially decomposed the original problem into two problems based on two potential decoding order schemes and then developed efficient algorithms utilizing the aforementioned methods to solve each transformed problem. Subsequently, the optimal solution to the original problem corresponds to the solution to the transformed problem yielding higher system EE. Simulation results have shown the quick convergence of the proposed algorithms and underscored the considerable advantages of our proposed scheme over other baseline schemes.

Several potential future directions are outlined below. First, further investigation is required into resource allocation strategies for relay-assisted CSR. Second, this work could be extended to scenarios where a non-linear energy harvesting model is implemented at the BN. Third, the resource allocation strategy should be redefined for PSR when incorporating reconfigurable intelligent surfaces as a replacement for a DF relay.

Author Contributions

All authors made significant contributions to this work. Xi Song performed the simulations and analyzed the results. Dongsheng Han contributed to drafting the manuscript. Liqin Shi provided the initial concept and solutions. Yinghui Ye assisted in writing and editing the manuscript. Xiaoli Chu offered critical revisions and participated in the final approval of the manuscript. All authors have read and approved the final manuscript.

Conflicts of Interest

The authors declare no conflicts of interest.

Data Availability Statement

The data that support the findings of this study are available from the corresponding author upon reasonable request.

References

1. X. Gao, D. Niyato, K. Yang, and J. An, "Cooperative Scheme for Backscatter-Aided Passive Relay Communications in Wireless-Powered D2D Networks," *IEEE Internet Things Journal* 9, no. 1 (2022): 152–164.

2. Z. Yang, M. Chen, Z. Zhang, and C. Huang, "Energy Efficient Semantic Communication Over Wireless Networks With Rate Splitting," *IEEE Journal on Selected Areas in Communications* 41, no. 5 (2023): 1484–1495.

3. J. Liu, J. Yu, D. Niyato, R. Zhang, X. Gao, and J. An, "Covert Ambient Backscatter Communications With Multi-Antenna Tag," *IEEE Transactions on Wireless Communications* 22, no. 9 (2023): 6199–6212.

4. X. Gao, P. Wang, D. Niyato, K. Yang, and J. An, "Auction-Based Time Scheduling for Backscatter-Aided RF-Powered Cognitive Radio Networks," *IEEE Transactions on Wireless Communications* 18, no. 3 (2019): 1684–1697.

5. B. Gu, D. Li, Y. Liu, and Y. Xu, "Exploiting Constructive Interference for Backscatter Communication Systems," *IEEE Transactions on Communications* 71, no. 7 (2023): 4344–4359.

6. C. Boyer, and S. Roy, "Backscatter Communication and Rfid: Coding, Energy, and Mimo Analysis," *IEEE Transactions on Communications* 62, no. 3 (2014): 770–785.

7. Y. Ye, L. Shi, X. Chu, G. Lu, and S. Sun, "Mutualistic Cooperative Ambient Backscatter Communications Under Hardware Impairments," *IEEE Transactions on Communications* 70, no. 11 (2022): 7656–7668.

8. Y. C. Liang, Q. Zhang, E. G. Larsson, , G. Y. Li, "Symbiotic Radio: Cognitive Backscattering Communications for Future Wireless Networks," *IEEE Transactions on Cognitive Communications and Networking* 6, no. 4 (2020): 1242–1255.

9. R. Long, , Y. C. Liang, H. Guo, G. Yang, and R. Zhang, "Symbiotic Radio: A New Communication Paradigm for Passive Internet of Things," *IEEE Internet of Things Journal* 7, no. 2 (2020): 1350–1363.

10. C. Zhou, B. Lyu, C. You, D. T. Hoang, "Cooperative Commensal and Parasitic Symbiotic Radio Communication Systems," *IEEE Wireless Communications Letters* 13, no. 3 (2024): 676–680.

11. Y. Ye, L. Shi, X. Chu, and G. Lu, "On the Outage Performance of Ambient Backscatter Communications," *IEEE Internet of Things Journal* 7, no. 8 (2020): 7265–7278.

12. G. Yang, T. Wei, and Y. C. Liang, "Joint Hybrid and Passive Beamforming for Millimeter Wave Symbiotic Radio Systems," *IEEE Wireless Communications Letters* 10, no. 10 (2021): 2294–2298.

13. H. Yang, Y. Ye, K. Liang, and X. Chu, "Energy Efficiency Maximization for Symbiotic Radio Networks With Multiple Backscatter Devices," *IEEE Open Journal of the Communications Society* 2 (2021): 1431–1444.

14. J. Xu, Z. Dai, and Y. Zeng, "Mimo Symbiotic Radio With Massive Backscatter Devices: Asymptotic Analysis and Precoding Optimization," *IEEE Transactions on Communications* 71, no. 9 (2023): 5487–5502.

15. M. Elsayed, A. Samir, A. A. A. E. Banna, X. Li, B. M. ElHalawany, "When Noma Multiplexing Meets Symbiotic Ambient Backscatter Communication: Outage Analysis," *IEEE Transactions on Vehicular Technology* 71, no. 1 (2022): 1026–1031.

16. H. Yang, H. Ding, and M. Elkashlan, "Opportunistic Symbiotic Backscatter Communication Systems," *IEEE Communications Letters* 27, no. 1 (2023): 100–104.

17. X. Song, D. Han, L. Shi, H. Sun, R. Q. Hu, "Relay Assisted Cooperative Ambient Backscatter Communication With Hybrid Long-Short Packets," *IEEE Transactions on Vehicular Technology* 73, no. 9 (2024): 12890–12903.

18. Z. Chu, W. Hao, P. Xiao, M. Khalily, and R. Tafazolli, "Resource Allocations for Symbiotic Radio With Finite Blocklength Backscatter Link," *IEEE Internet of Things Journal* 7, no. 9 (2020): 8192–8207.

19. H. Guo, Y. C. Liang, R. Long, and Q. Zhang, "Cooperative Ambient Backscatter System: A Symbiotic Radio Paradigm for Passive IoT," *IEEE Wireless Communications Letters* 8, no. 4 (2019): 1191–1194.

20. H. Guo, Y. C. Liang, R. Long, S. Xiao, and Q. Zhang, "Resource Allocation for Symbiotic Radio System With Fading Channels," *IEEE Access* 7 (2019): 34333–34347.

21. M. Nie, D. Mishra, A. A. nahari, J. Yuan, R. JÃd'ntti, "QoS Aware Transmit Beamforming for Secure Backscattering in Symbiotic Radio Systems," *IEEE Systems J* 18, no. 2 (2024): 1356–1367.

22. C. Jin, Z. Chang, F. Hu, H. H. Chen, and T. HÃd'mÃd'lÃd'inen, "Enhanced Physical Layer Security for Full-Duplex Symbiotic Radio With AN Generation and Forward Noise Suppression," *IEEE Transactions on Communications* 72, no. 7 (2024): 3905–3918.

23. B. Lyu, C. Zhou, S. Gong, W. Wu, D. T. Hoang, and D. Niyato, "Energy-Efficiency Maximization for STAR-RIS Enabled Cell-Free Symbiotic Radio Communications," *IEEE Transactions on Cognitive Communications and Networking* (2024): 1–1.

24. H. Zhou, B. Cai, Q. Zhang, R. Long, Y. Pei, Y. C. Liang, "Modulation design and optimization for RIS-assisted symbiotic radios," *IEEE Transactions on Wireless Communications* 23, no. 10 (2024): 13022–13038.

25. M. Wu, X. Lei, and D. B da Costa, "STAR-RIS-Assisted Full-Duplex Symbiotic Radio," *IEEE Wireless Communications Letters* 13, no. 11 (2024): 2945–2949.

26. J. Wang, Y. C. Liang, and S. Sun, "Multi-User Multi-IoT-Device Symbiotic Radio: A Novel Massive Access Scheme for Cellular IoT," *IEEE Transactions on Wireless Communications* 23, no. 9 (2024): 11876–11889.

27. W. Zhou, L. Shi, Y. Ye, X. Song, H. Sun, and G. Zheng, "Performance Analysis for Relay-Assisted Short-Packet Backscatter Communications," *IEEE Internet of Things Journal* 11, no. 17 (2024): 28988–29000.

28. Z. B. Zawawi, Y. Huang, and B. Clerckx, "Multiuser Wirelessly Powered Backscatter Communications: Nonlinearity, Waveform Design, and SINR-Energy Tradeoff," *IEEE Transactions on Wireless Communications* 18, no. 1 (2019): 241–253.

29. X. Gao, L. Shi, Y. Ye, G. Zheng, and G. Lu, "Reliability-Oriented Resource Allocation in Short-Packet Backscatter Communications," *IEEE Transactions on Vehicular Technology* 74, no. 2 (2025): 3468–3473.

30. W. Dinkelbach, "On Nonlinear Fractional Programming," *Management Science* 13, no. 7 (1967): 492–498.

31. S. Boyd and L. Vandenberghe, *Convex Optimization* (Cambridge University Press, 2004).